Structure Effects on the Ionicity of Protic Ionic Liquids

Sarah K. Mann,[b] Steven P. Brown,[b] and Douglas R. MacFarlane*[a]

[a] D. R. MacFarlane
School of Chemistry
Monash University
Clayton, 3168, Vic, Australia
E-mail: douglas.macfarlane@monash.edu
[b] S. K. Mann, S. P. Brown
Department of Physics
University of Warwick
Coventry, CV4 7AL, U.K.

Abstract: We report on the characterisation of 16 protic ionic liquids (PILs) prepared by neutralization of primary or tertiary amines with a range of simple carboxylic acids, or salicylic acid. The extent of proton transfer was greater for simple primary amine ILs compared to tertiary amines. For the latter case, proton transfer was increased by providing a better solvation environment for the ions through the addition of a hydroxyl group, either on the tertiary amine, or by formation of PIL/molecular solvent mixtures. The library of PILs was characterised by DSC and a range of transport properties (i.e. viscosity, conductivity and diffusivity) were measured. Using the (fractional) Walden rule, the conductivity and viscosity results were analysed with respect to their deviation from ideal behaviour. The validity of the Walden plot for PILs containing ions of varying sizes was also verified for a number of samples by directly measuring self-diffusion coefficients using pulsed-field gradient spin-echo (PGSE) NMR. Ionicity was found to decrease as the alkyl chain length and degree of branching of both the cations and anions was increased. These results aim to develop a better understanding of the relationship between PIL properties and structure, to help design ILs with optimal properties for applications.

Introduction

Ionic liquids (ILs), which are salts with melting points below 100 °C, have attracted interest in a broad range of fields due to their unique characteristics and large potential for tuning and optimising their properties for specific applications.[1] This traditional "salt" definition (i.e. consisting solely of ions) is best fulfilled by the aprotic ionic liquids (AILs), which consist of well-defined anions and cations. However, there are a number of important sub-classes of ILs, including protic ionic liquids (PILs), solvate ILs and metal complex-based ILs, that are characterised by dynamic equilibria involving neutral species. ~~There are two main classes of ILs, aprotic ionic liquids (AILs) and protic ionic liquids (PILs). AILs, the most frequently studied class, typically involve organic cations such as imidazoliums, pyridiniums and phosphoniums.~~ PILs, the focus of this work, are formed through transfer of a proton from a Brønsted acid (HA) to a Brønsted base (B), according to Equation 1:[2]

$$HA + B \rightleftharpoons BH^+ + A^- \qquad (1)$$

The properties of PILs are largely dependent on their degree of ionisation, however, the extent to which proton transfer occurs is not yet completely understood. The aqueous pK_a values for the acid and base, which determine the equilibrium constant for the proton transfer reaction in dilute aqueous solution, are not directly applicable to neat acid-based mixtures.[3] Yoshizawa *et al.* observed that a $\Delta pK_a > 10$ was required for complete proton transfer to occur, whilst in aqueous solution, $\Delta pK_a = 4$ gives 99% proton transfer.[3] The extent of proton transfer will depend on the structure of the acid and base constituents and their solvation ability. Stoimenovski *et al.* demonstrated that simple primary amines were able to deprotonate an indicator acid to a greater extent compared to tertiary amines with similar pK_a values.[4]

Many active pharmaceutical ingredients (APIs) are organic acids or bases that have the ability to form salts. In 2007, Rogers and co-workers described the reformulation of APIs as ILs.[5] Stoimenovski *et al.* reacted pharmaceutically active acids with pharmaceutical/biologically compatible bases to produce PILs.[6] Converting a neutral drug to a salt form can lead to improvements in the drug's properties, such as its solubility, absorption, pharmacodynamics and pharmacokinetics. Whilst there are a number of benefits of IL pharmaceuticals, it is well known that ionic drugs do not readily cross biological membranes and skin. However, it has been shown that some ~~protic~~ PILs exhibit enhanced membrane permeation, hypothesized to be due to the formation of neutral hydrogen-bonded clusters.[7] Stoimenovski *et al.* proposed that the formation of tetrameric clusters composed of two cations and two anions in primary amine containing PILs were responsible for decreased ionicity and enhanced membrane transport.[6-7] Similar cyclic tetramer hydrogen-bonding arrangements have been observed in molecular liquids such as propanol.[8] Recently, it was confirmed by infrared (IR) spectroscopy that theoretically predicted like-charge, hydrogen-bonded complexes exist in ionic liquids, showing that cooperative hydrogen bonding can compete with repulsive Coulombic forces.[8] Earlier studies by Kohler *et al.* on the interactions of amine and carboxylic acid mixtures also suggested the presence of hydrogen-bonded clusters.[9] For the case of a primary amine, butylamine, and propanoic acid, a complex of approximately four ion pairs with at least partial zwitterionic character was reported. The formation of clusters is present in some ILs but not others, despite similar structure of the cations and/or anions. For example, heptylammonium acetate appears to behave as freely dissociated ions, despite possessing the same functional groups (primary amine and carboxylic acid) as tuammoniumheptane salicylate, a PIL that forms hydrogen-bonded clusters.[6-7] A greater understanding of the factors that drive the formation of such clusters could enable the smart design of cluster-forming IL pharmaceuticals with improved membrane transport properties.

Angell and co-workers[10] described a convenient means to assess the ionicity and the presence of ion ~~pairs or other~~ correlations, using the Walden plot of log(molar conductivity, Λ_m)

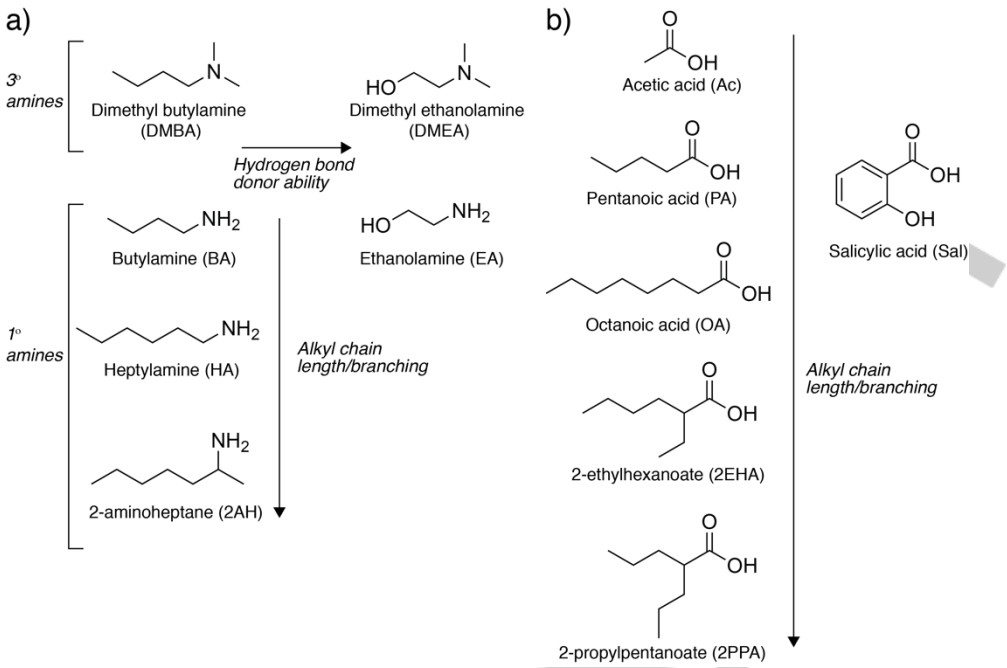

Scheme 1. Structures of a) primary amine and tertiary amine bases and b) acids with varying hydrogen-bonding ability and alkyl chain length and branching used in this study.

versus log(reciprocal viscosity, η^{-1}). The Walden rule, originally proposed for dilute electrolyte solutions, predicts a straight line passing through the origin, as expressed by Equation 2:

$$\log \Lambda_m = \log C + \log \eta^{-1} \qquad (2)$$

where C is a constant. Typically, a 0.01M KCl solution is used as a calibration point, and other electrolytes may be placed on the Walden plot for comparison with this "ideal" behaviour. In a 0.01M KCl solution, it is thought that the ions are well dissociated and approximately equally mobile. Deviations from the ideal line may be quantified by measuring the vertical distance, termed ΔW. A ΔW of 1 indicates that the IL exhibits 10% of the ionic conductivity that it would exhibit if it behaved according to the 0.01M KCl line. Whilst most ILs fall below the line,[10c, 11] it is in fact quite surprising that many ILs actually lie as close to the ideal line as they do, given that strong ion correlations are expected to a much greater extent in a pure salt, compared to a dilute aqueous solution. Such correlations may involve ion pairs (cation-anion), like-charge correlations (anion-anion and cation-cation) or larger clusters of multiple anions and cations. Significant research has focused on understanding the position of ILs on the Walden plot.[12] More detailed models based on Walden's rule have been proposed, such as the adjusted Walden plot and the fractional Walden rule, used in this work. By introducing an additional exponent, α, in Equation 3, a fractional Walden rule is obtained that allows the slope of the Walden plot to vary and more closely describe the temperature dependence that is typically seen in Walden plot data.[13]

$$\log \Lambda_m = \log C' + \alpha \log \eta^{-1} \qquad (3)$$

A more quantitative measure of the ionicity may be obtained from the ionic self-diffusion coefficients, using pulsed-field gradient spin-echo (PGSE) NMR. Using the Nernst-Einstein (NE) relation shown in Equation 4, the molar conductivity, Λ_{NE}, can be calculated from the measured diffusion coefficients:

$$\Lambda_{NE} = \frac{F^2}{RT}\left(v_+ z_+ D_+ + v_- z_- D_-\right) \qquad (4)$$

where F is the Faraday's constant, R is the universal gas constant, T is the temperature, v_+ and v_- are the number of cations and anions per unit formulae, z_+ and z_- are the cation and anion charge, and D_+ and D_- are the diffusion coefficients of the cation and anion, respectively. and Δ is the NE deviation parameter. The molar conductivity ratio, $\Lambda_{imp}/\Lambda_{NE}$ compares the conductivity obtained from impedance spectroscopy measurement (Λ_{imp}) to that calculated from NMR diffusivity measurements using the Nernst-Einstein relation (Λ_{NE}) and represents the proportion of ions that contribute to ionic conduction from the diffusing species. This may also be described by $\Delta I = \log_{10}(\Lambda_{NE}/\Lambda_{imp})$, providing a quantity analogous to ΔW determined from the Walden plot for comparison.

The proton conduction mechanism, in which charge transport occurs through molecular diffusion, as implied by the Walden and NE equations, is termed the vehicular mechanism. Proton hopping within hydrogen-bonded networks provides an alternative mechanism (the "Grotthuss mechanism", originally proposed for water) of conduction that is independent of the ion diffusion[14]. A mixture of Grotthuss-type and vehicular-mechanisms has been suggested to account for the proton conduction of some PILs,[15] including those composed of amine and carboxylic acids.[9]

The investigated PILs in this paper are based on primary and tertiary amine cations and simple carboxylic acid, or salicylic acid anions and their structures are shown in Scheme 1. ILs offer advantages in their tunability, which lead to the term "designer solvents",[16] however due to the complex nature of the possible interionic interactions[17] (i.e. Coulomb forces, dispersive interactions, π···π stacking, hydrogen bonding, *etc.*),

Table 1. PILs synthesised in this study.

	PIL	Abbreviation	RT form	T_g / °C	$T_{s\text{-}s}$ / °C	T_m / °C
1	Dimethyl butylamine Pentanoate	[DMBA][PA]	Liquid	-[a]	-	−45.03 ± 0.05
2	Dimethyl ethanolamine Pentanoate	[DMEA][PA]	Liquid	−71.6 ± 0.7	-	-
3	Butylamine Pentanoate	[BA][PA]	Liquid	-	-	-
4	Ethanolamine Pentanoate	[EA][PA]	Liquid	−73.7 ± 0.6	-	-
5	Heptylamine Acetate[4]	[HA][Ac]	Liquid	NA[b]	NA[b]	NA[b]
6	Heptylamine Pentanoate	[HA][PA]	Liquid	−88.0 ± 0.3	−16.65 ± 0.01	−5.06 ± 0.4
7	Heptylamine Octanoate	[HA][OA]	Supercooled liquid	-	3.76 ± 0.05, 14.91 ± 0.02	24.65 ± 0.2
8	Heptylamine 2-ethylhexanoate	[HA][2EHA]	Liquid	−78 ± 1	-	-
9	Heptylamine 2-propylpentanoate	[HA][2PPA]	Liquid	−75 ± 3	-	-
10	2-aminoheptane Pentanoate	[2AH][PA]	Liquid	−80 ± 1	-	-
11	2-aminoheptane Octanoate	[2AH][OA]	Supercooled liquid	-	−1.64 ± 0.01, −15.6 ± 0.4, 24.8 ± 0.3	31.0 ± 0.3
12	2-aminoheptane 2-ethylhexanoate	[2AH][2EHA]	Gel	-	-	-
13	2-aminoheptane 2-propylpentanoate	[2AH][2PPA]	Gel	-	-	-
14	Butylamine Salicylate	[BA][Sal]	Liquid	−60.6 ± 0.26	-	-
15	Heptylamine Salicylate	[HA][Sal]	Liquid	−55 ± 2	-	-
16	2-aminoheptane Salicylate[6]	[2AH][Sal]	Liquid	−62.5 ± 0.3	-	-

[a] "-" indicates that the transition was not observed by DSC over the temperature range studied. [b] DSC not measured.

aspects of structure do not easily translate to predictable changes in properties or function. The series of acids and bases in this work were chosen to investigate the influence of structure on the properties of PILs, and differ in their hydrogen bonding ability, alkyl chain length and degree of branching. There is recent interest in the use of IL/molecular solvent mixtures to further tune the properties of ILs.[18] A greater understanding of the interaction of PILs with molecular solvents will benefit many applications. Here, we show that the addition of hydrogen bonding solvents to a poorly ionized tertiary amine PIL can increase the degree of proton transfer and alter the transport properties including viscosity, conductivity and diffusivity.

Results and Discussion

Overview and Thermal Properties

16 different protic salts were synthesized by neutralization of primary or tertiary amines with a range of simple carboxylic acids, or salicylic acid (Sal). Of these, heptylamine acetate and 2-aminoheptane salicylate have been reported previously by Stoimenvoski *et al.*[4, 6-7] The acids and bases used in this study varied in their chain length, degree of alkyl chain branching, and presence of hydroxyl group. Their structures and abbreviations are shown in Scheme 1, and the protic salts synthesised in this work are summarised in Table 1. Of the 16 compounds synthesized, two formed gels ([2AH][2EHA] and [2AH][2PPA]) and two existed as either supercooled liquids or glassy solids at room temperature ([HA][OA] and [2AH][OA]), whilst the remaining 14 were RT liquids. The two gels were formed by the only PILs synthesised that contained both a branched cation (2AH) and branched anion (2EHA or 2PPA). Ionic liquid gels may be advantageous for certain applications, as not only do they retain the specific properties of ILs, they also gain the functional benefits associated with a semi-solid structure. As these gels were not the focus of this work and measuring the transport properties of such materials is challenging, no further investigation into the samples was performed. Whilst initially forming RT liquids, the octanoate PILs ([HA][OA] and [2AH][OA]) slowly crystallised at RT (over a period of several hours), indicating that they had initially formed supercooled liquids.

The phase behaviour was investigated by differential scanning calorimetry (DSC), and their glass transition temperatures (T_g), solid-solid phase transition temperatures ($T_{s\text{-}s}$), and melting points (T_m) are given in Table 1, while the DSC traces are shown in Figure 1. Only [DMBA][PA], [HA][PA], [HA][OA] and [2AH][OA] showed crystallisation and melting events. Notably, [HA][PA], [HA][OA] and [2AH][OA] underwent multiple ~~solid-solid~~ phase transitions ~~before melting.~~ This complex phase behaviour could be solid-solid phase transitions before melting, characteristic of plastic crystals, where the rotational motion of one or both of the ions in the crystal

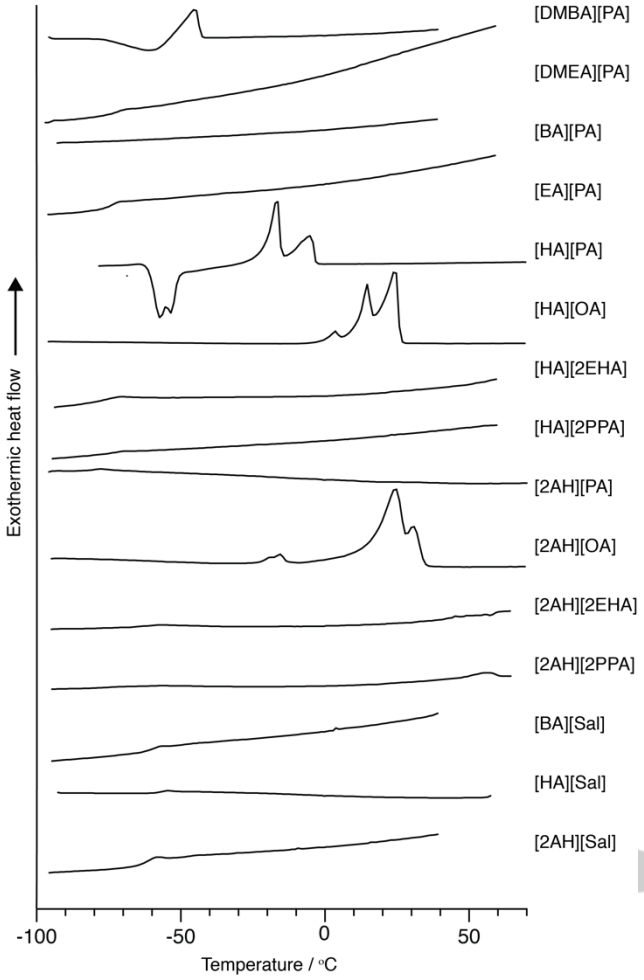

Figure 1. DSC thermograms of PILs at a heating rate of 10 °C min^{-1}.

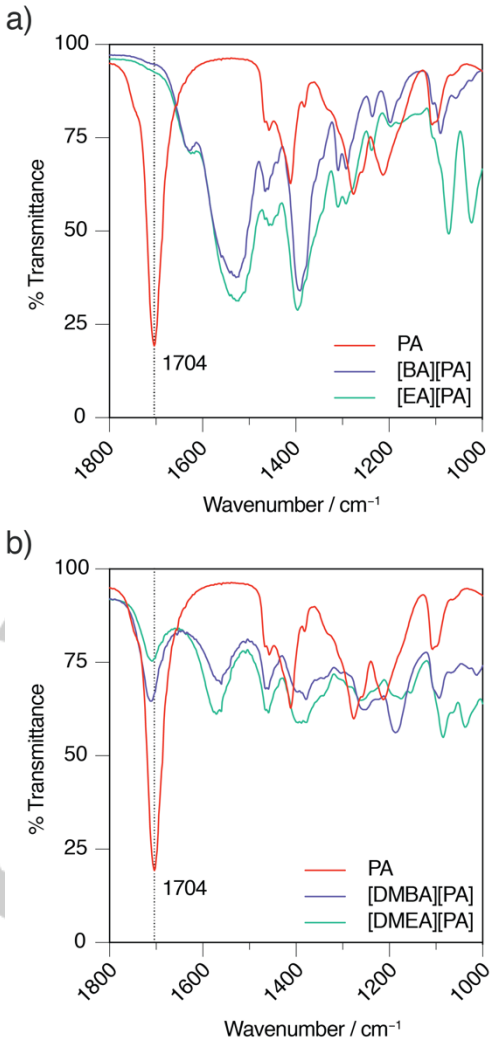

Figure 2. FTIR spectra of (a) pentanoic acid (red), [BA][PA] (purple) and [EA][PA] (green) and (b) pentanoic acid (red), [DMBA][PA] (purple) and [DMEA][PA] (green).

structure is released or could indicate the presence of a mixture of co-existing salt and acid/base components.

Influence of hydrogen bonding groups in primary and tertiary amine-based PILs and PIL/molecular solvent mixtures

We now turn our discussion to the ILs composed of either tertiary or primary amine bases with or without the presence of a hydroxyl group, combined with pentanoic acid (PILs 1-4 in Table 1). The pentanoate-based samples were all RT liquids, for both tertiary and primary amine bases with or without a hydroxyl functional group (Table 1). The properties of PILs depend largely on their degree of proton transfer. In neat PILs, the solvation environment has a very strong effect on the energy of proton transfer. Stoimenovski *et al.* showed that whilst primary amines tend to produce highly ionised ILs, the simple tertiary amine-based ILs of their study showed a low degree of proton transfer, attributable to the differences in hydrogen bonding environments offered by the amine/ammonium ions.[4, 19] They suggested that this trend may be easily disturbed by the presence of other functional groups, especially –OH or other hydrogen bonding sites. Indeed, in a later study, they found that the proton transfer behaviour of ILs containing the tertiary amine cation, 2-pyrrolidinoethanol, (EtOH)pyr, produced a significantly higher degree of proton transfer compared to the simple tertiary amines, presumably as a result of the hydroxyl group.[6] In order to investigate the degree of proton transfer, we recorded FTIR spectra of the PILs and the pentanoic acid starting material (Figure 2). The C=O stretch of pentanoic acid at 1704 cm^{-1} is absent in the primary amine PILs, ([BA][PA]) and [EA][PA]) (Figure 2a), which is indicative of complete ionisation ~~proton transfer~~. The ionic species may be involved in dynamic hydrogen-bonds of the form $A^{-}\cdots H{-}B^{+}$, which can be considered to lie on the proton transfer coordinate,[20] described by the equilibrium in Equation 1. A strong peak corresponding to the C=O stretch of the carboxylic acid is present in the spectra of the simple tertiary amine PIL, [DMBA][PA] (Figure 2b), indicating poor proton transfer, as expected. This system can therefore be considered an acid-base-IL mixture, with the equilibrium likely involving hydrogen-bonds of the form A–H···B and, to a smaller extent, $A^{-}\cdots H{-}B^{+}$. For the tertiary amine containing hydroxyl PIL, ([DMEA][PA]), the C=O stretch is still present albeit with reduced intensity relative to the other peaks, suggesting that, whilst not being complete, a higher degree of proton transfer has occurred compared to the simple tertiary amine PIL. The addition of a

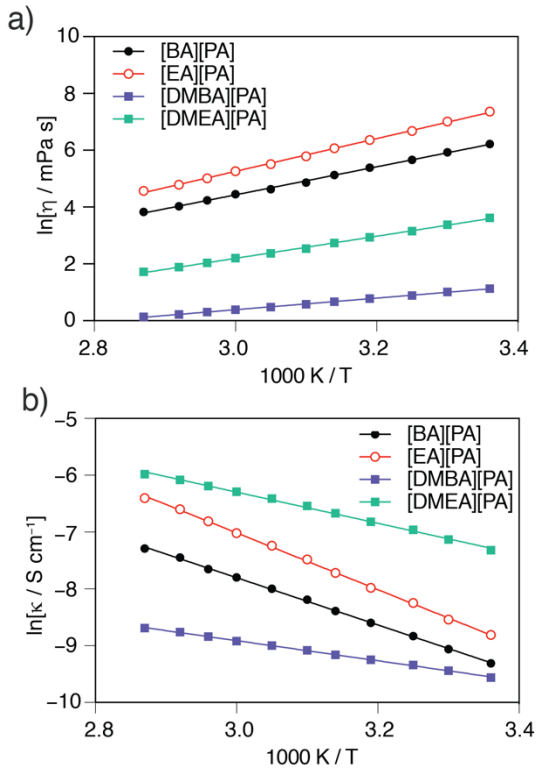

Figure 3. *units in y-axis label in b corrected* Arrhenius plots for pentanoate ILs temperature-dependence a) viscosity and b) conductivity data.

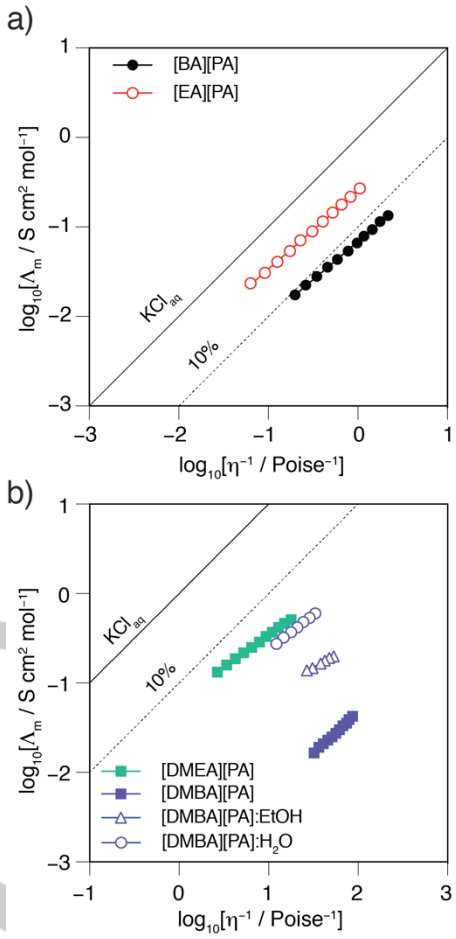

Figure 4. Walden plot of temperature-dependent conductivities and viscosities of a) primary amine and b) tertiary amine PILs and tertiary amine PIL/molecular solvent mixtures.

hydroxyl group to the amine as a hydrogen-bond donor can promote proton transfer by stabilising the carboxylate anion.

Viscosity and conductivity data are presented in Figure 3. Both plots show that the investigated PILs have Arrhenius-like behaviour. Table 2 summarises the Arrhenius fit parameters for viscosity data and conductivity data in Equations 5 and 6, respectively:

$$\eta = \eta_{\infty} \exp\left(\frac{E_{A,\eta}}{RT}\right) \quad (5)$$

$$\kappa = \kappa_{\infty} \exp\left(\frac{-E_{A,\kappa}}{RT}\right) \quad (6)$$

where $E_{A,\eta}$ is the apparent activation energy for viscous flow (i.e. the energy barrier that must be overcome for the ions to move past each other), η_{∞} is the maximum dynamic viscosity, $E_{A,\kappa}$ is the apparent activation energy indicating the energy required for an ion to hop into a free hole, κ_{∞} is the maximum electrical conductivity, R is the gas constant, and T is the temperature in Kelvin. Equations 5 and 6 are not expected to hold over extended temperatures ranges where curvature in the Arrhenius plot would indicate the need to use a VTF form of fitting function, however, the measured data did not show sufficient curvature to warrant the use of the additional fitting parameter.

The primary amine-based pentanoate PILs possess viscosities more than an order of magnitude higher than the tertiary amine based PIL, consistent with both the stronger ionic interactions in the more highly ionized systems and additional hydrogen-bonding possible in the primary amine-based systems, which contain multiple hydrogen-bond donors (Figure 3a). Of the primary amine based PILs, the hydroxyl containing [EA][PA] is more viscous than its simple amine analogue, [BA][PA], which may be attributed to the additional hydrogen bonding involving the hydroxyl group. Similarly, the tertiary amine-based PIL [DMEA][PA] is more viscous than the simple amine [DMBA][PA], as a result of the higher degree of ionisation and additional hydrogen bonding of the hydroxyl group. $E_{A,\eta}$ for [DMBA][PA] is significantly lower at 17.0 kJ mol^{-1}, compared to the other three PILs with apparent activation energies for viscous flow above 30 kJ mol^{-1} (Table 2), consistent with a lower energy barrier for viscous flow due to weaker electrostatic interactions. η_{∞} was also significantly different for [DBMA][PA], more than two orders of magnitude higher compared to the other PILs (Table 2). η_{∞} is representative of a structural contribution of the ions to the viscosity, since interactions that contribute to the viscosity are no longer effective at infinite temperature.

The ionic conductivities also show distinct differences between the four PILs (Figure 3b), which cannot be attributed to differences in the viscosities alone. The simple tertiary amine-based PIL, [DMBA][PA], shows the lowest conductivity, despite its low viscosity, consistent with a low degree of proton transfer. The hydroxyl functionalised analogue, [DMEA][PA], showed a significant improvement in conductivity, showing higher conductivity than both primary amine-based ILs, despite the

Table 2. Arrhenius fit parameters for the viscosity (Equation 5) and conductivity (Equation 6) data presented in Figure 3 and for fractional Walden plots (Equation 3) presented in Figure 4.

	Viscosity		Conductivity			Walden	
PIL	$10^4 \times \eta_\infty$ / mPa s	$E_{A,\eta}$ / kJ mol^{-1}	κ_∞ / S cm^{-1}	$E_{A,\kappa}$ / kJ mol^{-1}	α	log(C' / S cm^2 mol^{-1})	ΔW (298 K)
[BA][PA]	0.31 ± 0.06	41.0 ± 0.5	[1.1 ± 0.1] × 10^2	34.6 ± 0.3	0.851 ± 0.007	−1.163 ± 0.002	1.1
[EA][PA]	0.06 ± 0.01	47.9 ± 0.5	[2.9 ± 0.4] × 10^3	41.5 ± 0.4	0.877 ± 0.006	−0.594 ± 0.004	0.43
[DMBA][PA]	32 ± 2	17.0 ± 0.2	0.027 ± 0.001	14.7 ± 0.1	0.93 ± 0.01	−3.18 ± 0.03	3.3
[DMEA][PA]	0.8 ± 0.1	32.3 ± 0.4	7 ± 1	22.8 ± 0.4	0.723 ± 0.005	−1.185 ± 0.005	1.3

$R^2 > 0.997$ for all linear fits.

lower degree of proton transfer and lower viscosity. As for the tertiary amine PILs, the presence of the hydroxyl group was shown to improve the conductivity for the primary amine-based PILs, with [EA][PA] showing a higher conductivity compared to the simple primary amine-based [BA][PA], despite being more viscous.

In order to further our understanding of the transport behaviour, the viscosity and conductivity data were combined into Walden plots (Figure 4). Fits to the fractional Walden rule (Equation 3) are given in Table 2. Notably, all of the fits produced α values in the range of 0.72-0.93, as is typically observed for a variety of ILs. Both the simple amine based PILs (primary amine [BA][PA]: Figure 4a, and tertiary amine [DMBA][PA]: Figure 4b) show a significant deviation from the ideal line, although to a much greater extent for [DMBA][PA], consistent with incomplete proton transfer as observed by FTIR. [BA][PA] lies just below the 10% line, despite IR showing complete ionisation ~~proton transfer~~. For both the primary and tertiary-based PILs, the presence of the hydroxyl group ([EA][PA]: Figure 4a and [DMEA][PA]: Figure 4b) results in a significantly closer agreement to the Walden rule compared to the simple amine-based PILs. This is expected for the tertiary amine-based PILs, since the FTIR spectra showed a higher degree of proton transfer for the hydroxyl functionalised PIL. It is less clear why this is the case for the primary amine PILs, where complete ionisation ~~proton transfer~~ has occurred in either case. This could suggest~~s~~ that the hydroxyl functionalised [EA][PA] displays a lower degree of association (i.e. less tendency to form ion pairs and clusters) compared to the simple amine [BA][PA], despite the additional hydrogen bonding ability. ~~This could be due to increased cation-cation hydrogen bond interactions leading to weaker cation-anion association.~~ The nature of like-ion (cation-cation and anion-anion) correlation affects has also been shown to strongly influence conductivity.[21] Such affects could result from increased cation-cation hydrogen-bond interactions of the ethanolamine ions, i.e. correlated motion, but may also be strongly influenced by the anticorrelated motion of ions. The ethanolamine cation also lacks the extended alkyl chain that is present in butylamine. As will be discussed below, the length of alkyl chains in PILs and the hydrocarbon-hydrocarbon interactions have a significant effect on the ionicity of PILs.

The closer to 'ideal' Walden behaviour for the hydroxyl-functionalised PILs could also be accounted for by a secondary Grotthuss-type hopping mechanism for proton transport. A key factor for proton transport via the Grotthuss mechanism is the presence of a hydrogen-bonded network, which is consistent with the increased viscosity observed for the hydroxyl-functionalised PILs. Deviations from the classical Walden rule, where proton conduction is coupled to translational diffusion and the slope, $\alpha = 1$, have previously been attributed to a Grotthuss-type transport mechanism in some PILs, such as lidocaine di-(dihydrogen phosphate), for which $\alpha = 0.53$ was reported.[15c] We note a significantly lower value of $\alpha = 0.723$ for the hydroxyl functionalized [DMEA][PA] compared to [DMBA][PA] ($\alpha = 0.93$) (Table 2), while the primary amine based PILs showed similar values ($\alpha = 0.851$ and 0.877). While these deviations from ideal behaviour could indicate a contribution of a mechanism aside from vehicle transport, $\alpha < 1$ could also reflect temperature-induced changes in the degree of proton transfer or ion association.

Combining ILs and molecular solvents has been shown to be a promising strategy for tuning properties, with a variety of applications reported to benefit from IL/solvent mixtures, so much so that they have recently been referred to as "a 4th Evolution of Ionic Liquids".[18] The properties of IL/solvent mixtures are not always predictable on the basis of simple mixing rules, but instead reflect interactions between the ionic and molecular components. Since the low degree of proton transfer in the tertiary amine ILs is due to its poor solvation environment, we combined the tertiary amine-based IL, [DMBA][PA], with stoichiometric quantities of hydrogen-bonding solvents (ethanol or H_2O). For the simple tertiary amine IL, [DMBA][PA], where poor proton transfer occurred, the addition of a hydrogen bonding solvent (ethanol or H_2O) promoted proton transfer as expected, however proton transfer was still not complete, as indicated by the presence of a carbonyl IR stretch at 1704 cm^{-1} (Figure 5). A significant increase in viscosity was observed on the addition of solvent, consistent with increased proton transfer and/or increased hydrogen bonding and was greater for H_2O compared to ethanol (Figure 6a).

The molar conductivity of both IL/solvent mixtures increased by more than ~~2~~ two orders of magnitude, with the H_2O mixture showing the highest conductivity, despite also being the most viscous (Figure 6b). Walden plots for the IL/molecular solvent

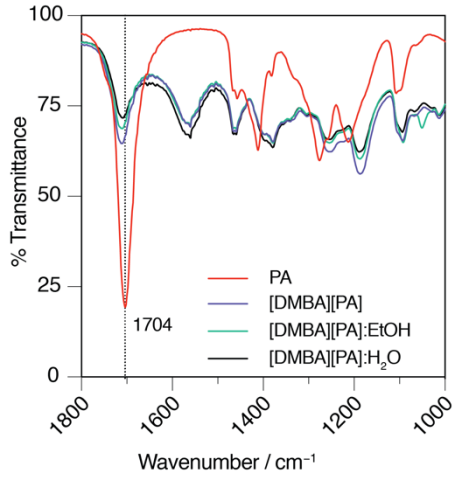

Figure 5. FTIR spectra of pentanoic acid (red), [DMBA][PA] (purple), [DMBA][PA]:EtOH (green) and [DMBA][PA]:H_2O (black).

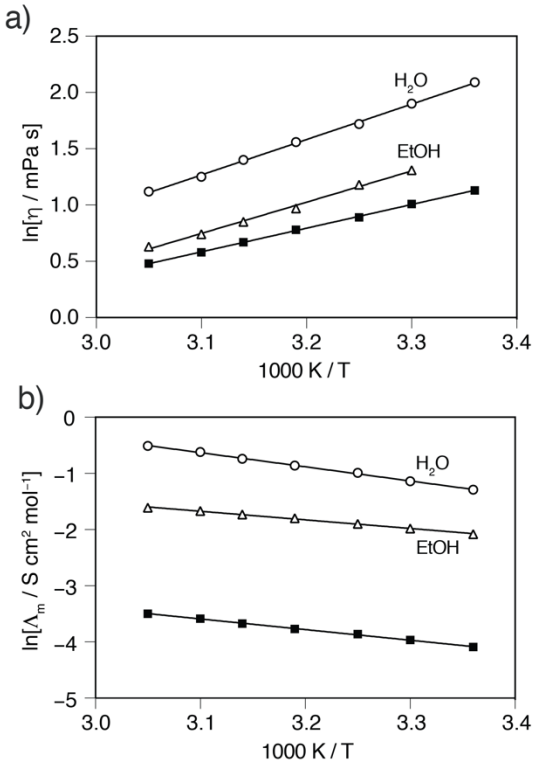

Figure 6. (a) Viscosity and (b) Molar conductivity data for [DMBA][PA] pure IL (closed squares) and IL/solvent mixtures (open symbols). Note that the molar conductivity is presented in (b) rather than the conductivity as displayed for other ILs, to account for the proportion of ionic and molecular species.

mixtures are shown in Figure 4b, alongside the tertiary amine-based ILs for comparison. The IL/molecular solvent mixtures appear closer to the 'ideal' line on the Walden plot compared to the pure IL. This is likely a result of increased ionicity due to stabilisation of the carboxylate anion by the hydroxyl proton in the same manner as the hydroxyl group in [DMEA][PA]. The addition of EtOH to [DMBA][PA], however, does not increase the ionicity compared to that of [DMEA][PA], despite both containing the same molar equivalents of the hydroxyl functional group. The difference in the Walden behaviour could be due to the butyl chain present in DMBA but not in DMEA, as will be discussed further below. The H_2O mixture appears closer to the Walden line, almost matching that of the hydroxyl functionalised [DMEA][PA], which may be attributed to the additional hydrogen bond donor ability of H_2O compared to EtOH. The Grotthuss-type proton conduction mechanism may also contribute to a greater extent in the IL/solvent mixtures, where an extended hydrogen-bonded network could result from the addition of the molecular solvents that can provide both hydrogen-acceptor and donor sites. Overall, these results show that the addition of hydrogen-bonding molecular solvents to ILs displaying poor proton transfer may be a viable strategy in order to improve ionicity.

Influence of alkyl chain-length and branching on the properties of primary amine-based PILs

In addition to the hydrogen bonding ability and presence of functional groups, the nature of non-polar regions (e.g. alkyl-length and degree of branching) can be expected to strongly influence the properties of PILs. The following discussion is on the PILs composed of either heptylamine (straight chain) or 2-aminoheptane (branched) primary amine bases, combined with five different acids of varying chain length and degree of branching: acetic acid, pentatonic acid, octanoic acid, 2-ethylhexanoic acid, and 2-propylpentanoic acid (PILs 5-13 in Table 1). In addition, we investigated the influence of the base chain length/degree of branching in three salicylate-based PILs paired with the simple primary amines, butylamine, heptylamine, or 2-aminoheptane (PILs 14-16 in Table 1).

Temperature-dependent densities, viscosities and conductivities were measured for all of the PILs, excluding the two gels, at temperatures from 298 to 348 K. All of the PILs showed Arrhenius viscosity and conductivity behaviour (Table 3). The temperature dependent viscosity of PILs containing a branched ion (either cation or anion), showed a steeper slope, indicating a larger apparent activation energy of viscous flow (Figure 7a and c, Table 3). The conductivities of the different primary amine salicylate PILs differ with the shorter butylammonium IL exhibiting the highest conductivity (Figure 7b), even though all the PILs appear to be completely proton transferred. Despite similar viscosities of the pentanoate and octanoate PILs with either heptylamine or 2-aminoheptane (note the crossover of curves at intermediate temperatures), significant differences in conductivities were observed (Figure 7c). The branched 2AH containing ILs showed lower conductivities compared to the straight chain HA ILs.

As expected, the Walden plot shows a linear temperature dependence for each PIL. [2AH][Sal] falls well below the "ideal line", as has been previously reported (Figure 8a),[6] indicating that the majority of the ions form neutral ion pairs or clusters which are unable to conduct. It was suggested (based on crystal structures of analogous compounds) that the ions organise into a cyclic hydrogen-bonded cluster-like complex consisting of two cations and two anions.[6] Despite also containing a primary amine, [HA][Sal] shows slightly closer to ideal behaviour, whilst [BA][Sal] shows even better agreement with the Walden rule (Figure 8a), suggesting that the formation of such clusters is not as common or are not as long-lived as for the 2AH containing PIL, or, additional factors influence the transport behaviour. Understanding the reasons for these differences may enable the design of ILs with a tendency to form strong hydrogen-bonded clusters. This is of particular importance since hydrogen-bonded

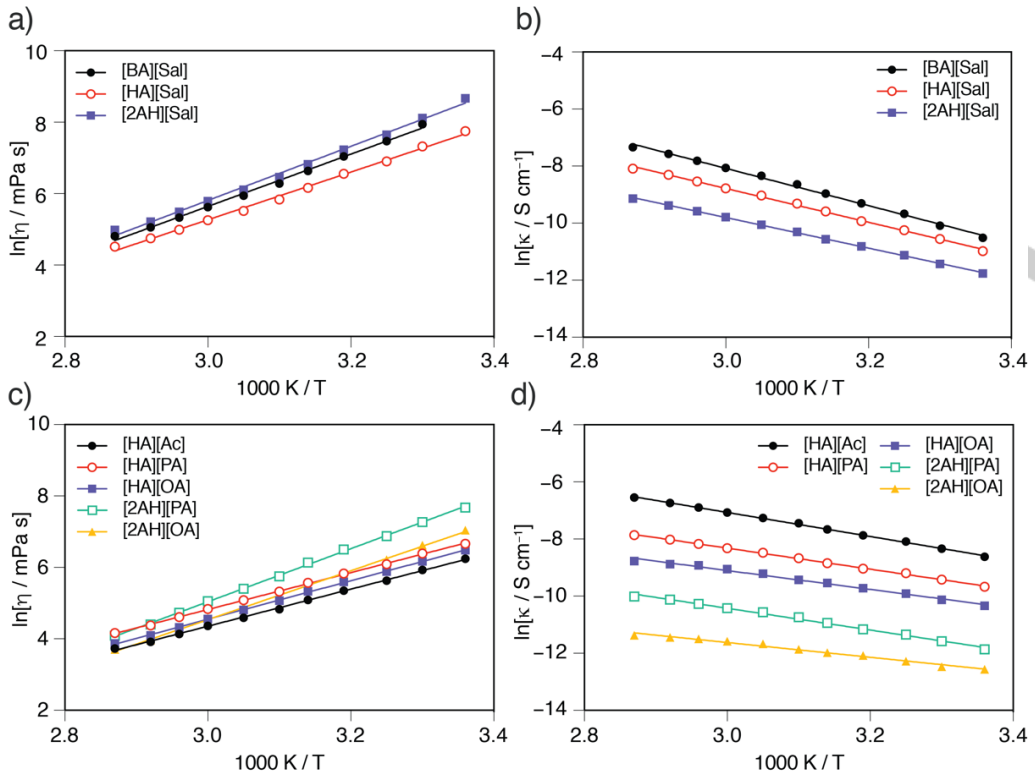

Figure 7. **units in y-axis label in b corrected** Arrhenius plots for salicylate PILs temperature-dependence (a, c) viscosity and (b, d) conductivity and acetate, pentanoate and octanoate PILs temperature-dependence (c) viscosity and (d) conductivity.

cluster forming ILs have been shown to transport much more readily through model membranes compared to dissociated PILs.[7]

[HA][Ac] lies close to the 10% line, as previously reported[4] (Figure 8b), whilst the PILs with increasing anion chain length show increased deviation from ideal behaviour following the trend octanoate > pentanoate > acetate (Figure 8b). Increasing the alkyl chain length decreases the molar concentration of the ions, leading to a decrease in the electrostatic attraction between cations and anions, whilst increasing van der Waals interactions of the alkyl chain-ion inductive forces and hydrocarbon-hydrocarbon interactions.

Molecular dynamics simulations and X-ray scattering experiments have demonstrated that when the length of alkyl tails increases beyond a critical length, nanophase segregation occurs in numerous ILs, where the charge-rich ionic regions and the charge-poor aliphatic regions cluster into domains.[22] For the frequently studied imidazolium class of AILs, X-ray diffraction studies showed a characteristic diffraction peak assigned to nonpolar alkyl chain aggregations for those ILs having alkyl chains of four or more carbon atoms. Ueno et al. reported that imidazolium ILs with one to two carbon atoms in the alkyl chain of the imidazolium showed similar ionicity, but ionicity began to decrease significantly on going from four to eight carbon atoms, confirming that the attraction between the nonpolar alkyl chain groups impacts on the ionicity of ILs.[23] Griffin et al. found that nanophase segregation of alkyl chains in a series of quaternary ammonium ILs reduces the ionicity due to aggregation-induced suppression of dynamics.[24] Nanostructure has also been observed for PILs containing an alkylammonium cation, where there are at least two carbon atoms in the alkyl chain.[25] In the pentanoate and octanoate PILs studied here, the van der Waals attraction between the nonpolar alkyl chains and possible segregation into domains could account for the extremely low

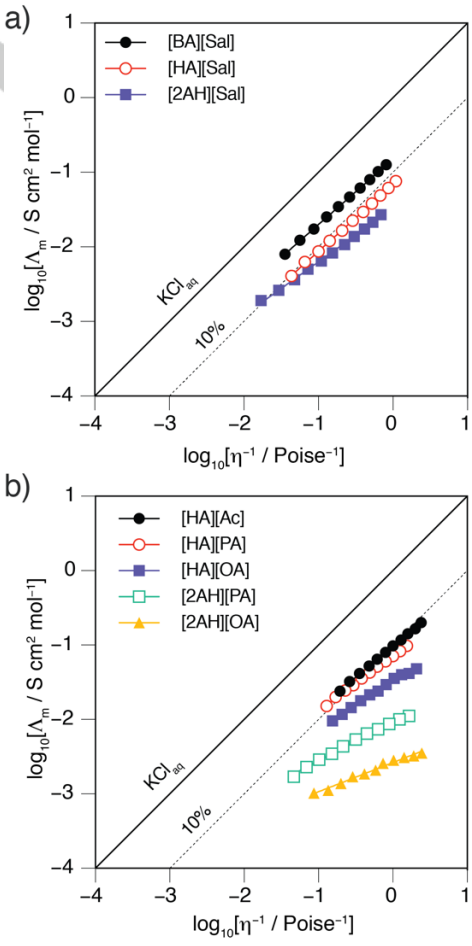

Figure 8. Walden plot of temperature-dependence conductivities and viscosities of a) salicylate PILs with varying primary amine cations and b) acetate, pentanoate and octanoate PILs.

Table 3. Arrhenius fit parameters for the viscosity (Equation 5) and conductivity (Equation 6) data presented in Figure 7 and for fractional Walden plots (Equation 3) presented in Figure 8.

	Viscosity		Conductivity			Walden	
PIL	$10^6 \times \eta_\infty$ / mPa s	$E_{A,\eta}$ / kJ mol^{-1}	κ_∞ / S cm^{-1}	$E_{A,\kappa}$ / kJ mol^{-1}	α	log(C' / S cm^2 mol^{-1})	ΔW (298 K)
[BA][Sal]	0.08 ± 0.04	61 ± 1	[1.0 ± 0.4] × 10^5	54 ± 1	0.879 ± 0.004	−0.821 ± 0.004	0.65 (303 K)
[HA][Sal]	0.4 ± 0.2	56 ± 1	[8 ± 2] × 10^3	49.3 ± 0.7	0.897 ± 0.006	−1.162 ± 0.005	1.02
[2AH][Sal]	0.04 ± 0.02	63 ± 1	[5.4 ± 0.8] × 10^2	44.6 ± 0.4	0.71 ± 0.01	−1.49 ± 0.01	0.96
[HA][Ac]	14 ± 2	43.1 ± 0.4	[2.6 ± 0.4] × 10^{-2}	35.0 ± 0.4	0.827 ± 0.007	−1.017 ± 0.003	0.90
[HA][PA]	23 ± 3	42.9 ± 0.4	15 ± 2	30.6 ± 0.4	0.734 ± 0.008	−1.146 ± 0.004	0.92
[HA][OA]	9 ± 1	44.8 ± 0.3	2.3 ± 0.7	27.5 ± 0.9	0.63 ± 0.02	−1.149 ± 0.007	1.21
[2AH][PA]	0.032 ± 0.007	61.8 ± 0.6	2.7 ± 0.8	31.7 ± 0.8	0.52 ± 0.01	−2.03 ± 0.01	1.43
[2AH][OA]	0.11 ± 0.03	56.9 ± 0.7	0.0021 ± 0.007	21.5 ± 0.8	0.39 ± 0.02	−2.578 ± 0.008	1.93

$R^2 > 0.99$ for all linear fits.

ionicity observed in the Walden plots. Further studies, such as X-ray diffraction, are required to confirm the presence of nanostructure in the PILs in this work.

As with the salicylate PILs, the branched 2-aminoheptane PILs paired with pentanoate and octanoate, showed poorer ionicity compared to those containing the straight chain heptylamine. [2AH][PA] and [2AH][OA] also showed a low values of α (= 0.52 and 0.39, respectively). The value of α reflects the difference of apparent activation energies of the ionic conductivity and viscosity and could reflect a temperature induced change in the degree of ion association or proton transfer.

The Walden plot provides a convenient means for comparing ionicity between ILs, however does not take into the effect of differing ion sizes. The effect of ion size can be considered by a corrected Walden plot adjusted using the calculated ionic radius as described by Bonhôte *et al*.[26] and Abbott,[27] or by directly measuring the diffusion, most commonly by means of PGSE NMR. We utilised the latter method and measured diffusion coefficients by PGSE-NMR to compare the molar conductivity to experimental diffusivity. Due to experimental difficulties measuring diffusion in highly viscous ILs (a combination of slow diffusion and fast relaxation), PGSE-NMR measurements were performed at 40 °C where the samples are significantly less viscous than at RT. The calculated $\Lambda_{imp}/\Lambda_{NE}$ and related $\Delta I = \log_{10}(\Lambda_{NE}/\Lambda_{imp})$ values for several ILs are given in Table 4, alongside ΔW obtained from the Walden plots. The excellent correlation between ΔW and ΔI indicate that the Walden plot is a reasonable measure of ionicity, both following the same trends, without requiring the more time-consuming PGSE-NMR measurements.

The relative diffusion coefficients of the acidic proton (D_{H+}) compared to those of the non-exchangeable protons of the cation and anion (D_+ and D_-, respectively) can provide information of the mechanism of proton conduction.[15b] An enhancement of D_{H+} compared to D_+ may result from intermolecular proton exchange (a Grotthuss-type mechanism), while similar values are expected for the case of vehicular transport. A value of D_{H+} 1.5 times higher than the heptylammonium cation was observed for [HA][Ac] (Table 4). Watanabe *et al*. proposed a Grotthuss-type proton conduction mechanism in the PIL composed of *N*-methylimidazole and acetic acid involving fast rotation of acetic acid/acetate as a key

Table 4. Diffusion coefficients from PGSE NMR for selected PILs. All reported values were recorded at 313 K.

IL	D_{cation} / m^2 s^{-1}	D_{anion} / m^2 s^{-1}	D_{H+} / m^2 s^{-1}	$\Lambda_{imp}/\Lambda_{NE}$	ΔI[a]	ΔW[a]
[HA][Ac]	4.4 × 10^{-12}	5.6 × 10^{-12}	6.5 × 10^{-12}	0.15	0.83	1.0~~0.96~~
[HA][PA]	4.4 × 10^{-12}	3.9 × 10^{-12}	4.9 × 10^{-12}	0.10	1.0	1.0
[2AH][Sal]	6.3 × 10^{-13}	6.5 × 10^{-13}	6.1 × 10^{-13}	0.11	1.0~~0.96~~	1.2
[2AH][PA]	2.6 × 10^{-12}	2.3 × 10^{-12}	2.7 × 10^{-12}	0.020	1.7	1.6
[2AH][OA]	3.2 × 10^{-12}	2.9 × 10^{-12}	3.7 × 10^{-12}	0.008	2.1	2.2

[a] The estimated errors in ΔI and ΔW are ± 0.1.

step.[28] A similar mechanism may contribute in [HA][Ac], accounting for the higher conductivity observed compared to the other PILs. For the remaining PILs, there was either a small enhancement of D_H compared to D_+ (D_{H+}/D_+= 1.1 and 1.2 for [HA][PA] and [2AH][OA], respectively) or no significant difference (D_{H+}/D_+= 1.0 for [2AH][Sal] and [2AH][PA]), consistent with the vehicular mechanism dominating the proton conductivity in these cases.

Conclusion

A series of PILs were prepared from a range of primary or tertiary amines, and carboxylic acids. Temperature-dependent physicochemical properties such as viscosity, density, and conductivity were measured, and Walden plots constructed to determine the ionicity of the PILs. The ionicities of the studied PILs vary with the systematic variation in the structure of the cations and anions. FTIR and Walden plot studies indicated that the tertiary amine-based PIL exhibited poor proton transfer in comparison to PILs containing primary amines, however improvement of the solvation ability by the addition of a hydroxyl group promoted proton transfer. In general, PILs containing either acids or bases with longer alkyl chain lengths and branched chains showed decreased ionicity. In addition, IL/molecular solvent mixtures were prepared from either water or ethanol, and the tertiary amine-based PIL, [DMBA][PA], which exhibited poor proton transfer in the pure IL form. The addition of the molecular solvent was shown to promote proton transfer, and lead to an increase in viscosity, conductivity and ionicity compared to the pure PIL, demonstrating that IL/molecular solvent mixtures are a promising strategy to tune the transport properties of PILs. PGSE-NMR measurements of ionicity showed good correlation between ΔW and ΔI, confirming that the former provides an accessible and realistic reflection of ion association effects.

Experimental Section

Sample preparation

All PILs were prepared by mixing equimolar amounts of the constituent acids and bases at room temperature and stirred for 2 h. The PILs were then dried at 40 °C on a Schlenk line (~0.3 torr) for a minimum of 3 h.

Measurement of thermal and transport properties

DSC scans were carried out at a heating/cooling rate of 10 °C min^{-1} using a Perkin Elmer DSC 8000. Transition temperatures are reported using the peak maximum of the thermal transition. The FTIR spectra were obtained using an Agilent FTIR spectrometer. Density measurements were carried out at different temperatures using an Anton Paar DMA5000 density meter. The dynamic viscosities were determined at temperatures matching the density measurements using a rolling ball viscosity meter (Anton Paar Lovis 2000ME). The ionic conductivities were measured by electrochemical impedance spectroscopy. A home-built dip cell consisting of two platinum wires sheathed in glass was immersed in the sample. The complex impedance spectra were measured over a frequency range of 100 MHz to 1 MHz. The temperature was controlled with a Eurotherm 2204E temperature control unit, a thermocouple and heating block holding the cell compartment. The cell constant was determined using a solution of 0.01 M KCl at 25 °C.

Diffusion coefficients were obtained from ^{1}H pulsed-field gradient stimulated spin-echo (PGSE) NMR experiments performed on a Bruker Avance III 600 MHz (9.4 T) spectrometer. D_2O in an external capillary was used as the lock solvent. The interval between gradient pulses, Δ, was set to 800 ms, and the length of the gradient pulse, δ, was 2.5 ms. 16 gradient strengths were used ranging from 1.70 to 32.4 T m^{-1}. 16 transients were co-added and a recycle delay of 3 s was used.

Acknowledgements

This research was supported by the Warwick Monash Alliance. Funding from GSK for a PhD studentship (SKM) is acknowledged. SKM is supported by a University of Warwick International Chancellor's scholarship. DRM acknowledges his Australian Laureate Fellowship from the Australian Research Council (FL120100019). The data for this study is provided as a supporting dataset from WRAP, the Warwick Research Archive Portal at http://wrap.warwick.ac.uk/*****/.

Keywords: protic ionic liquids • proton transfer • viscosity • conductivity • ionicity

[1] N. V. Plechkova, K. R. Seddon, *Chem. Soc. Rev.* **2008**, *37*, 123-150.
[2] T. L. Greaves, C. J. Drummond, *Chem. Rev.* **2008**, *108*, 206-237.
[3] D. R. MacFarlane, J. M. Pringle, K. M. Johansson, S. A. Forsyth, M. Forsyth, *ChemComm.* **2006**, 1905-1917.
[4] J. Stoimenovski, E. I. Izgorodina, D. R. MacFarlane, *Phys. Chem. Chem. Phys.* **2010**, *12*, 10341-10347.
[5] W. L. Hough, M. Smiglak, H. Rodríguez, R. P. Swatloski, S. K. Spear, D. T. Daly, J. Pernak, J. E. Grisel, R. D. Carliss, M. D. Soutullo, J. J. H. Davis, R. D. Rogers, *New Journal of Chemistry* **2007**, *31*, 1429-1436.
[6] J. Stoimenovski, P. M. Dean, E. I. Izgorodina, D. R. MacFarlane, *Faraday Discuss.* **2012**, *154*, 335-352.
[7] J. Stoimenovski, D. R. MacFarlane, *ChemComm.* **2011**, *47*, 11429-11431.
[8] A. Knorr, P. Stange, K. Fumino, F. Weinhold, R. Ludwig, *Chemphyschem* **2016**, *17*, 458-462.
[9] a) F. Kohler, H. Atrops, H. Kalali, E. Liebermann, E. Wilhelm, F. Ratkovics, T. Salamon, *The Journal of Physical Chemistry* **1981**, *85*, 2520-2524; b) F. Kohler, R. Gopal, G. Goetze, H. Atrops, M. Demeriz, E. Liebermann, E. Wilhelm, F. Ratkovics, B. Palagyi, *The Journal of Physical Chemistry* **1981**, *85*, 2524-2529.
[10] a) C. A. Angell, N. Byrne, J.-P. Belieres, *Acc. Chem. Res.* **2007**, *40*, 1228-1236; b) W. Xu, E. I. Cooper, C. A. Angell, *J. Phys. Chem. B* **2003**, *107*, 6170-6178; c) M. Yoshizawa, W. Xu, C. A. Angell, *J. Am. Chem. Soc.* **2003**, *125*, 15411-15419.
[11] C. Zhao, G. Burrell, A. A. J. Torriero, F. Separovic, N. F. Dunlop, D. R. MacFarlane, A. M. Bond, *J. Phys. Chem. B* **2008**, *112*, 6923-6936.
[12] D. R. MacFarlane, M. Forsyth, E. I. Izgorodina, A. P. Abbott, G. Annat, K. Fraser, *Phys. Chem. Chem. Phys.* **2009**, *11*, 4962-4967.
[13] C. Schreiner, S. Zugmann, R. Hartl, H. J. Gores, *J. Chem. Eng. Data* **2010**, *55*, 1784-1788.
[14] a) N. Agmon, *Chemical Physics Letters* **1995**, *244*, 456-462; b) K.-D. Kreuer, *Chemistry of materials* **1996**, *8*, 610-641.
[15] a) M. Anouti, J. Jacquemin, P. Porion, *J. Phys. Chem. B* **2012**, *116*, 4228-4238; b) A. Noda, M. A. B. H. Susan, K. Kudo, S. Mitsushima, K. Hayamizu, M. Watanabe, *J. Phys. Chem. B* **2003**, *107*, 4024-4033; c) Z. Wojnarowska, Y. Wang, K. J. Paluch, A. P. Sokolov, M. Paluch, *Phys. Chem. Chem. Phys.* **2014**, *16*, 9123-9127.
[16] M. Freemantle, *Chem. Eng. News* **1998**, *76*, 32-37.
[17] a) S. Zahn, F. Uhlig, J. Thar, C. Spickermann, B. Kirchner, *Angew. Chem. Int. Ed.* **2008**, *47*, 3639-3641; b) P. A. Hunt, C. R. Ashworth, R. P. Matthews, *Chem. Soc. Rev.* **2015**, *44*, 1257-1288.
[18] D. R. MacFarlane, A. L. Chong, M. Forsyth, M. Kar, R. Vijayaraghavan, A. Somers, J. M. Pringle, *Faraday Discuss.* **2018**, *206*, 9-28.
[19] K. M. Johansson, E. I. Izgorodina, M. Forsyth, D. R. MacFarlane, K. R. Seddon, *Phys. Chem. Chem. Phys.* **2008**, *10*, 2972-2978.
[20] T. Steiner, *Angew. Chem. Int. Ed.* **2002**, *41*, 48-76.

[21] N. M. Vargas‐Barbosa, B. Roling, *ChemElectroChem* **2020**, *7*, 367-385.
[22] a) R. Hayes, G. G. Warr, R. Atkin, *Chem. Rev.* **2015**, *115*, 6357-6426; b) J. N. A. Canongia Lopes, A. A. H. Pádua, *J. Phys. Chem. B* **2006**, *110*, 3330-3335; c) A. Triolo, O. Russina, H.-J. Bleif, E. Di Cola, *J. Phys. Chem. B* **2007**, *111*, 4641-4644; d) Y. Wang, G. A. Voth, *J. Phys. Chem. B* **2006**, *110*, 18601-18608.
[23] K. Ueno, H. Tokuda, M. Watanabe, *Phys. Chem. Chem. Phys.* **2010**, *12*, 1649-1658.
[24] P. J. Griffin, Y. Wang, A. P. Holt, A. P. Sokolov, *J. Phys. Chem.* **2016**, *144*, 151104.
[25] a) R. Atkin, G. G. Warr, *J. Phys. Chem. B* **2008**, *112*, 4164-4166; b) T. L. Greaves, D. F. Kennedy, S. T. Mudie, C. J. Drummond, *J. Phys. Chem. B* **2010**, *114*, 10022-10031.
[26] a) P. Bonhôte, A.-P. Dias, M. Armand, N. Papageorgiou, K. Kalyanasundaram, M. Grätzel, *Inorg. Chem.* **1998**, *37*, 166-166; b) P. Bonhôte, A.-P. Dias, N. Papageorgiou, K. Kalyanasundaram, M. Grätzel, *Inorg. Chem.* **1996**, *35*, 1168-1178.
[27] A. P. Abbott, *ChemPhysChem* **2005**, *6*, 2502-2505.
[28] H. Watanabe, T. Umecky, N. Arai, A. Nazet, T. Takamuku, K. R. Harris, Y. Kameda, R. Buchner, Y. Umebayashi, *J. Phys. Chem. B* **2019**, *123*, 6244-6252.

Entry for the Table of Contents

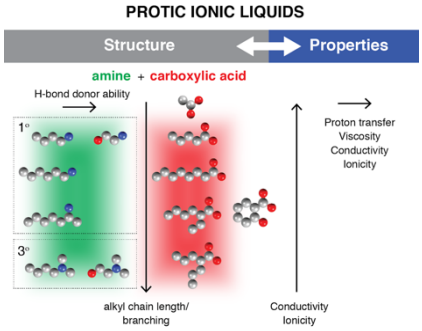

Protic ionic liquids (PILs) based on primary or tertiary amine cations and simple carboxylic acid anions, or salicylic acid, have been synthesised and characterised, revealing the influence of structural aspects (hydrogen bonding ability, alkyl chain length and degree of branching) on the transport properties and ionicity.

Institute and/or researcher Twitter usernames: @DRMacFarlane